Optical Materials: X 7 (2020) 100056

Contents lists available at ScienceDirect

Optical Materials: X

journal homepage: www.journals.elsevier.com/optical-materials-x

SiO_2-SnO_2:Er^{3+} planar waveguides: Highly photorefractive glass-ceramics

Thi Ngoc Lam Tran [a,b,c,*], Simone Berneschi [d], Cosimo Trono [d], Gualtiero Nunzi Conti [d], Lidia Zur [b], Cristina Armellini [b], Stefano Varas [b], Alessandro Carpentiero [b], Andrea Chiappini [b], Alessandro Chiasera [b], James Gates [e], Pier-John Sazio [e], Monica Bollani [a], Anna Lukowiak [f], Giancarlo C. Righini [d], Maurizio Ferrari [b]

[a] IFN-CNR, P.zza Leonardo da Vinci, 20133, Milano, Italy
[b] IFN-CNR CSMFO Lab. and FBK Photonics Unit, Via alla Cascata 56/C, 38123, Povo, Italy
[c] Department of Materials Technology, Faculty of Applied Sciences, Ho Chi Minh City University of Technology and Education, Vo Van Ngan Street 1, Thu Duc District, 720214, Ho Chi Minh City, Viet Nam
[d] MiPLab, IFAC-CNR, Via Madonna del Piano 10, 50019, Sesto Fiorentino, Italy
[e] ORC, Optoelectronics Research Centre, University of Southampton, University Road, Southampton, SO17 1BJ, UK
[f] Institute of Low Temperature and Structure Research, PAS, ul. Okólna 2, 50422, Wroclaw, Poland

ARTICLE INFO

Keywords:
Photorefractivity
Direct UV writing
Grating inscription
SiO_2-SnO_2 glass-ceramics
Erbium
Sol-gel

ABSTRACT

For different applications in laser photonics and integrated optics, photorefractive materials are surely of great interest and play an important role in miniaturization of devices and fabrication of functional photonic structures such as gratings and waveguides. In this work, high photorefractivity of sol-gel derived SiO_2-SnO_2:Er^{3+} glass-ceramic planar waveguides, with negative effective refractive index change, is demonstrated. Through the photorefractivity investigation employing the UV pulsed KrF excimer laser (λ = 248 nm), the glass-ceramic planar waveguides show fast photorefractive response after a cumulative dose of only 0.3 kJ/cm^2. A higher SnO_2 content in the glass-ceramics leads to a greater change of saturated effective refractive index: Δn_{eff} = - (2.60 ± 0.20) x 10^{-3} at 1550 nm on the TE_0 mode, for the 30 mol% SnO_2 planar waveguides and Δn_{eff} = - (2.00 ± 0.20) x 10^{-3} on the 1550 nm TE_0 mode, for the 20 mol% SnO_2 ones. To investigate the structural modifications involved in the photorefractivity of the SiO_2-SnO_2:Er^{3+} glass-ceramics, XRD and Raman characterizations are employed. The grating fabrication by direct UV writing on the SiO_2-SnO_2:Er^{3+} glass-ceramic planar waveguide as well as an important reduction in the employed energy is demonstrated.

1. Introduction

Thanks to the role of tin dioxide (SnO_2) as rare-earths luminescence sensitizer, SnO_2-SiO_2 glass-ceramics with a broad transparency window (UV–Vis–NIR) are demonstrated to be an appealing candidate for the development of efficient luminescent glass-based photonic systems such as microcavities, solid state lasers, integrated optical amplifiers, and optical sensors [1–3]. Besides this feature, the SiO_2-SnO_2 glass-ceramics also exhibit an additional interesting characteristic: photorefractivity [4,5], which makes them unique and innovative for many application areas such as integrated optics and laser photonics. Therefore, these binary SiO_2-SnO_2 systems have drawn a special attention to numerous researches not only on the development of luminescent structures [1–3,6,7] but also on the exploitation of the photorefractivity [4,5,8,9].

Briefly, the photorefractivity potential of tin dioxide-based glasses was first realized in tin-codoped germanosilicate [10] and phosphosilicate [11,12] optical fibers. By introducing tin in such silicate glasses, the strong photorefractivity gratings fabricated by UV irradiation with enhanced refractive index change up to ~1.2–1.4 × 10^{-3} was obtained. Some of the first studies on the photorefractivity of the single tin-doped silicate were in forms of fiber [10,13,14]. The results showed a comparable refractive index change with less consumed SnO_2 based silicate glasses compared to GeO_2 based silicate glasses, a well-known class of strong photorefractive materials used for Fiber Bragg gratings and integrated optics [15]. Moreover, in comparison with GeO_2 based silicate glasses, since SnO_2 based silicate glasses exhibit high photorefractivity, they do not need post-processes for photorefractivity enhancement such as hydrogen-loading which is time-consuming and high induced-losses

* Corresponding author. IFN-CNR, P.zza Leonardo da Vinci, 20133, Milano, Italy.
E-mail address: thitran@fbk.eu (T.N.L. Tran).

https://doi.org/10.1016/j.omx.2020.100056
Received 27 May 2020; Accepted 25 June 2020
Available online 15 July 2020

at 1.5 μm region [13]. In addition, SnO_2-SiO_2 fibers potentially provide a lower numerical aperture and higher thermal stability [14]. These appealing features have led to numerous researches on the development of photorefractive SiO_2-SnO_2 systems by several methods such as MCVD [13], melt quenching [16], and ion-implantation methods [17]. However, in general these approaches have encountered several limitations of low SnO_2 content, α-Sn nanoclusters and nonstoichiometric SnO_x nanoparticles.

Recently, sol-gel has been shown as a profitable fabrication method to produce these specific photonic materials with high SnO_2 content [3,18,19] thanks to its low temperature and melt-free synthesis, and ease of multicomponent fabrication [3]. The sol-gel derived SiO_2-SnO_2 glass-ceramics were studied both in form of monoliths [20–22] and thin films [3,18,19,23–25].

Most of the studies of the photorefractivity of this glass-ceramic was focused on the monolithic forms with low SnO_2 content (up to 5 mol%) [26,27]. The works [9,26–29] placed the first bricks for the photorefractivity investigation under UV irradiation in these binary systems: positive refractive index change for the substitutional tin-doped silica glasses and negative refractive index change for the SiO_2-SnO_2 glass-ceramics. In particular, the work [27] reported a negative refractive index change of 10^{-4} as order of magnitude in the SiO_2-SnO_2 glass-ceramics containing only 5 mol% SnO_2. In our prior publications [4,7,8], we demonstrated that high photorefractivity (negative refractive index change in the order of 10^{-3}) could be obtained in the sol-gel derived SiO_2-SnO_2 glass-ceramic waveguides with high SnO_2 content (25 mol%). The volume expansion and polarizability were suggested to contribute to the change of refractive index. With this large UV-induced refractive index change, SiO_2-SnO_2 glass-ceramics are promising for efficient top-down fabrication of channel waveguides and Bragg gratings. In this consolidated work, we demonstrate the high and fast response of the photorefractivity of the sol-gel derived SiO_2-SnO_2 glass-ceramic planar waveguides with a special attention to the impact of SnO_2 content. XRD and Raman characterizations are employed to understand the structural modification involved in the photorefractivity of the SiO_2-SnO_2:Er^{3+} glass-ceramics. Furthermore, the first result of UV-written grating fabrication on the SiO_2-SnO_2:Er^{3+} planar waveguide is also demonstrated and shows its energy-efficient aspect in comparison with GeO_2 based silicate glasses, e.g. hydrogen loaded germanoborosilicate glasses.

2. Materials and methods

2.1. Sol-gel derived planar waveguides

The photorefractivity of (100-x)SiO_2-xSnO_2:yEr^{3+} planar waveguides (x, y: mol%) is explored on two glass-ceramic compositions (20 and 30 mol% SnO_2) doped with the same concentration of Er^{3+} (0.5 mol %) as listed in Table 1.

Table 1
The compositions of the (100-x)SiO_2-xSnO_2:yEr^{3+} planar waveguides with $\mathbf{x} = \frac{100 \times \mathbf{n}_{\mathbf{SnO_2}}}{\mathbf{n}_{\mathbf{SnO_2}} + \mathbf{n}_{\mathbf{SiO_2}}}$(mol%) and $\mathbf{y} = \frac{100 \times \mathbf{n}_{\mathbf{Er^{3+}}}}{\mathbf{n}_{\mathbf{SnO_2}} + \mathbf{n}_{\mathbf{SiO_2}}}$ (mol%) where $n_{Er^{3+}}$,n_{SnO_2} and n_{SiO_2} are molar concentration of Er^{3+}, SnO_2 and SiO_2 respectively.

Sample notation	Composition		
	SnO_2 content (x: mol%)	SiO_2 content (100-x: mol%)	Er^{3+} concentration (y: mol%)
70SiO_2-30SnO_2:0.5Er^{3+}	30	70	0.5
80SiO_2-20SnO_2:0.5Er^{3+}	20	80	0.5

All the samples were fabricated by sol-gel method and dip-coating technique. The sol-gel derived fabrication of the SiO_2-SnO_2:Er^{3+} glass-ceramic planar waveguides can be summarized by three different steps: (i) solution synthesis, (ii) dip-coating and intermediate drying step for each single layer and (iii) final heat-treatment for the deposited multilayer planar waveguides. The details of the solution synthesis, dip-coating deposition and heat-treatment were reported in our previous publication [1]. After the final heat-treatment at 1000 °C for 1 h in air, transparent SiO_2-SnO_2:Er^{3+} glass-ceramic planar waveguides were obtained with a thickness of about 1.3 ± 0.1 μm. In addition, SiO_2-SnO_2:Er^{3+} glass-ceramic planar waveguides were embedded by SnO_2 nanocrystals with size of less than 10 nm, which was already reported along with other structural characterizations in our recent work [1].

2.2. Photorefractivity investigation: the experimental set-ups

A KrF excimer laser at 248 nm (Lambda Physik Compex 110, Coherent Inc., Santa Clara, CA, USA) was employed for the photorefractivity investigation of the SiO_2-SnO_2:Er^{3+} planar waveguides. Fig. 1 shows the setup scheme for the UV irradiation. After successive reflections through a series of three mirrors, the laser beam reached the target section. This was represented by a black metal panel, on which there was a square slit of around 1 cm × 1 cm. The sample surface was masked with an aluminum sheet, having a square aperture with a size close to that of the slit adopted for the UV irradiation. The specimen was positioned and fixed on the back of the black panel (with respect to the laser beam inlet direction), taking care to align these two masks (the metal mask for the UV irradiation on the panel and the mask represented by the aluminum sheet on the sample). To test the photorefractive response of the planar waveguides under UV irradiation, the adopted pulse fluence (i.e.: the laser pulse energy per unit of area) was 30 mJ/cm^2. For both samples, the first cumulative dose of 22.5 J/cm^2 was achieved with a repetition rate of 10 Hz. Afterwards, a repetition rate of 50 Hz was employed to obtain the final cumulative dose of 9.0 kJ/cm^2 and ensure the attainment of the saturated effective refractive index change of the samples.

For the effective refractive index measurements of the modes supported by the planar waveguides, a home-made instrument based on prism coupling technique developed in IFAC-CNR, Sesto Fiorentino, Italy, with a nominal resolution on the measured effective refractive index of about 5 × 10^{-5} was used The measurements were performed before and after each UV exposure at 1550 nm. Statistical measurements were carried out with a repetition of 7 times by removing and inserting the sample in the coupling region (i.e.: the aperture of the aluminum sheet) with the prism. In this way, the standard deviation on the mode effective refractive index measurement was determined to be: 2 × 10^{-4}.

2.3. Characterization of the irradiated planar waveguides

After the last exposure, the planar waveguides were characterized with different techniques. XRD and Raman characterizations were employed to understand the structural modification involved in the photorefractivity of the SiO_2-SnO_2:Er^{3+} glass-ceramics. The X-ray diffraction patterns were acquired using X'PERT PRO diffractometer equipped with a Cu X-ray tube. Moreover, to check the structural modification, the micro-Raman spectra were acquired using Labram Aramis (Horiba Jobin-Yvon) equipped with an optical microscope, a 100 × objective and a He-Ne laser (632 nm) as the excitation source.

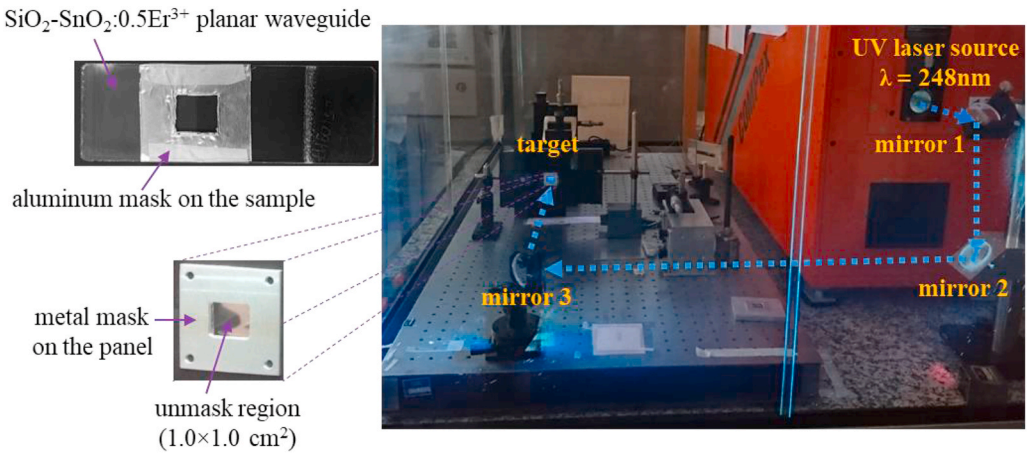

Fig. 1. Experimental setup of the UV irradiation for the photorefractivity measurements.

2.4. Gratings inscription

On the basis of the above-mentioned photorefractivity investigation, the photorefractive 70SiO_2-30SnO_2:0.5Er^{3+} planar waveguide was chosen for fabricating UV-direct written gratings. For such gratings fabrication, a CW frequency doubled argon laser (λ = 244 nm) with a writing fluence of 1.0 kJ/cm^2 was employed. Using a ~5 μm MFD (Mode-field diameter) spot, the gratings formed with 5 μm pitch raster pattern over 4 × 4 mm^2 area were fabricated on a piece of the sample.

3. Results and discussion

3.1. Negative effective refractive index changes of the planar waveguides

After UV irradiation, both glass-ceramic planar waveguides exhibited negative effective refractive index change. Fig. 2 shows the effective refractive index change of the fundamental 1550 nm TE_0 mode of the 70SiO_2-30SnO_2:0.5Er^{3+} planar waveguide as a function of the cumulative dose. From this figure, one can see that the 70SiO_2-30SnO_2:0.5Er^{3+}glass-ceramic planar waveguide showed a very fast photorefractive response: after the first dose of 0.003 kJ/cm^2, the effective refractive index of the 1550 nm TE_0 mode already presented a significant change of - (1.10 ± 0.20) × 10^{-3}. The change in the 1550 nm TE_0 effective refractive index reached its saturated value of - (2.60 ± 0.20) × 10^{-3} after a UV cumulative dose of only 0.3 kJ/cm^2. The inset

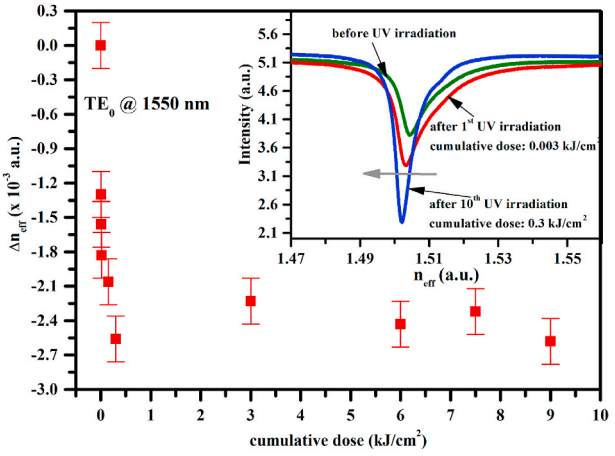

Fig. 2. Effective refractive index changes on 1550 nm TE_0 mode supported by the 70SiO_2-30SnO_2:0.5Er^{3+} planar waveguide as a function of cumulative dose. The inset image is the shift to the lower index values of the 1550 nm TE_0 mode after the two UV cumulative doses: 0.003 kJ/cm^2 (the 1st UV irradiation) and 0.3 kJ/cm^2 (the 10th UV irradiation).

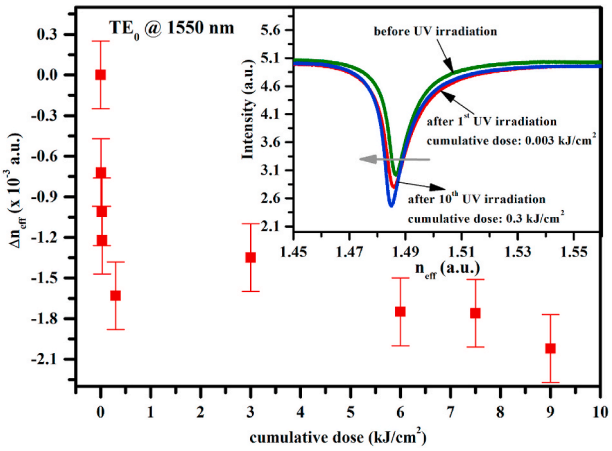

Fig. 3. Effective refractive index changes on 1550 nm TE_0 mode supported by the 80SiO_2-20SnO_2:0.5Er^{3+} planar waveguide as a function of cumulative dose. The inset image is the shift to the lower index values of the 1550 nm TE_0 mode after the two UV cumulative doses: 0.003 kJ/cm^2 (the 1st UV irradiation) and 0.3 kJ/cm^2 (the 10th UV irradiation).

image in Fig. 2 reveals the corresponding shift to the lower index values of 1550 nm TE_0 mode after these two UV cumulative doses: 0.003 kJ/cm^2 (the 1st UV irradiation) and 0.3 kJ/cm^2 (the 10th UV irradiation).

A negative effective refractive index change on 1550 nm TE_0 mode was also obtained after UV irradiation in the 80SiO_2-20SnO_2:0.3Er^{3+} planar waveguide as shown in Fig. 3. A fast effective refractive index change was also observed. After the first dose of 0.003 kJ/cm^2, the effective refractive index had a significant decrease of - (0.70 ± 0.20) × 10^{-3}. And, after a cumulative dose of only 0.3 kJ/cm^2, it reached rapidly the value of - (1.6 ± 0.20) × 10^{-3} which was nearly 80% of its saturated effective refractive index change of - (2.00 ± 0.20) × 10^{-3}. The shift to lower values of the 1550 nm TE_0 mode effective refractive index change is revealed in the inset image of Fig. 3.

The changes of the overall UV-induced effective refractive index of the 1550 nm TE_0 mode supported by the two planar waveguides are respectively summarized in Table 2.

Table 2 shows that higher SnO_2 content in the glass-ceramic planar

Table 2
The overall UV-induced effective refractive index changes of the fundamental 1550 nm TE_0 mode supported by the 70SiO_2-30SnO_2:0.5Er^{3+} and 80SiO_2-20SnO_2:0.5Er^{3+} planar waveguides.

Sample	Δn_{eff}
70SiO_2-30SnO_2:0.5Er^{3+}	- (2.60 ± 0.20) x 10^{-3}
80SiO_2-20SnO_2:0.5Er^{3+}	- (2.00 ± 0.20) x 10^{-3}

waveguides leads to higher photorefractivity: the effective refractive index measured at 1550 nm on TE_0 mode changes of - (2.6 ± 0.2) × 10^{-3} for the 30 mol% SnO_2 planar waveguide and of - (2.0 ± 0.2) × 10^{-3} for the 20 mol% SnO_2 planar waveguide. This behavior is in agreement with the work [25] on germanium-free tin doped silica thin films deposited by helicon activated reaction evaporation process (HARE).

In our prior work [4], the negative effective refractive index change of the SiO_2-SnO_2:Er^{3+} glass-ceramic planar waveguides was suggested to be a consequence of a volume expansion and polarizability change of the material. However, to understand the involved structural factors in the photorefractive response in the SiO_2-SnO_2:Er^{3+} glass-ceramics, the structural characterization of the planar waveguides before and after UV irradiation was carried out. In the literature, in terms of structural modification of SnO_2:SnO_2 binary systems induced by UV irradiation, two factors have been suggested to be involved in the photorefractive response: (i) phase change of SnO_2 nanoclusters according to the work [27], and (ii) the breaking of network bonds due to Sn-doping as observed in the works [30,31]. To scope the change of SnO_2 crystallinity as well as SiO_2 phase of the glass-ceramic planar waveguide after UV irradiation, XRD characterization was employed. Concerning the characterization of the network bonds in the system, micro-Raman spectroscopy was used.

3.2. Characterization of the irradiated planar waveguides

3.2.1. XRD

Fig. 4 shows the XRD patterns of the 70SiO_2-30SnO_2:0.5Er^{3+} planar waveguide before and after UV irradiation. The two patterns exhibit a broad band centered at 22° of amorphous SiO_2 and some relevant XRD peaks at 26, 34, 52° indexed as the planes (110), (101) and (211) of SnO_2-rutile Cassiterite (JCPDS 41–1445). By means of XRD patterns, no noticeable structural change of the SiO_2-SnO_2:Er^{3+} glass-ceramic planar waveguide after UV irradiation in terms of SnO_2 crystallinity and amorphous phase of SiO_2 was revealed.

3.2.2. Micro-Raman

Although the XRD patterns show no remarkable changes of SnO_2 crystallinity and SiO_2 amorphous phase, a change in the structure of the SiO_2-SnO_2 glass-ceramic is revealed by Raman spectroscopy. Fig. 5 shows the micro-Raman spectra (λ_{ex} = 632 nm) of the 70SiO_2-30SnO_2:0.5Er^{3+} planar waveguide before and after UV irradiation. In the Raman spectrum of the irradiated planar waveguide, there is the presence of a fluorescence background which was also observed in the literature [30]. This fluorescence background was suggested to relate to the network modification existing due to the presence of SnO_2 in SiO_2 matrix [30,31]. However, to define exact mechanisms and microscopic origins that drive the photorefractivity of such materials, further structural investigation is demanded, and this is beyond the scope of this paper.

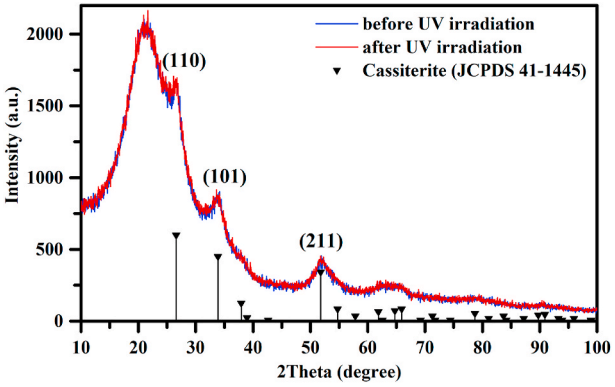

Fig. 4. XRD patterns of the 70SiO_2-30SnO_2:0.5Er^{3+} planar waveguide before and after UV irradiation, indexed as SnO_2 Cassiterite (JCPDS 41–1445).

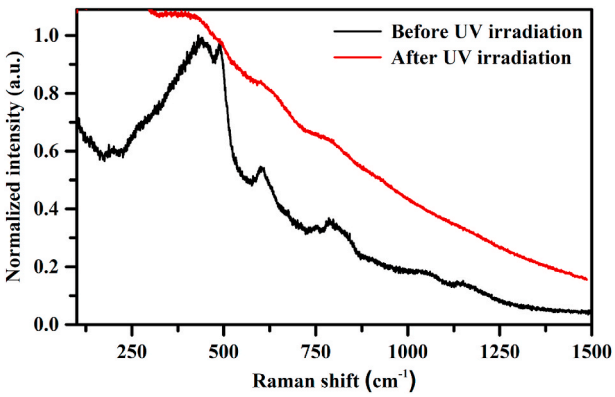

Fig. 5. Micro-Raman spectra (λ_{ex} = 632 nm) of the 70SiO_2-30SnO_2:0.5Er^{3+} planar waveguide before and after UV irradiation.

3.3. Gratings inscription

For the first time, the optical gratings were fabricated in the highly photorefractive SiO_2-SnO_2 glass-ceramic planar waveguides (with 30 mol% SnO_2) activated by Er^{3+}. Fig. 6 shows the gratings formed with 5 μm pitch raster pattern over 4 × 4 mm^2 on a small piece of the 70SiO_2-30SnO_2:0.5Er^{3+} planar waveguide, fabricated by a CW frequency doubled argon laser (λ = 244 nm). This is a proof of concept of gratings inscription using direct UV writing thanks to the high photorefractivity of the SiO_2-SnO_2:Er^{3+} glass-ceramic planar waveguides.

Moreover, after a writing fluence of 1.0 kJ/cm^2, a high average refractive index variation over the grating's region of 4.3 × 10^{-3} was measured via a prism coupling technique at 1550 nm. A comparison with the gratings fabrication on hydrogen loaded germanium doped silica glasses in the work [32] shows that the 70SiO_2-30SnO_2:0.5Er^{3+} planar waveguide exhibits a faster photorefractive response. To obtain a refractive index change in the order of 10^{-3}, the energy density needed

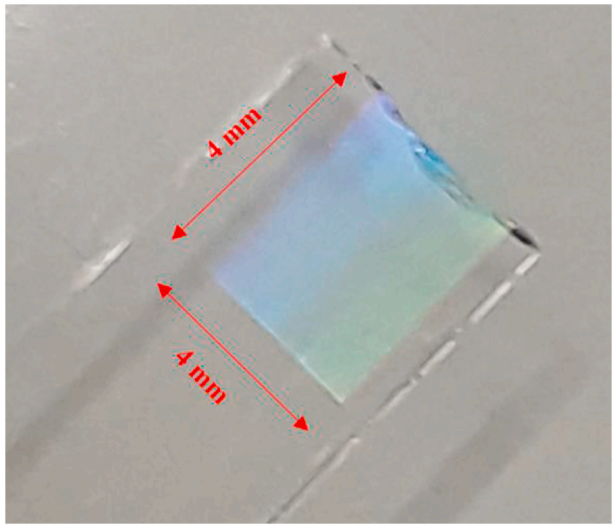

Fig. 6. Image of the optical gratings fabricated by a CW frequency doubled argon laser λ = 244 nm with a writing fluence of 1.0 kJ/cm^2 on a 4 × 4 mm^2 area of the 70SiO_2-30SnO_2:0.5Er^{3+} glass-ceramic planar waveguide. One can see the colors due to the interference patterns scattering from the gratings based on the Bragg law. (For interpretation of the references to color in this figure legend, the reader is referred to the Web version of this article.)

for hydrogen loaded germanoborosilicate glasses was 12.0 kJ/cm^2 [32], i.e. one order of magnitude greater than for the SiO_2-SnO_2:Er^{3+} glass-ceramic planar waveguide. In other words, this energy-efficient aspect of the direct UV-written gratings on the SiO_2-SnO_2:Er^{3+} glass-ceramics results in less time-consuming fabrication processes compared with germanoborosilicate glasses. Therefore, the highly photorefractive SiO_2-SnO_2 glass-ceramics can be an appealing candidate for the development of optical integrated components. Furthermore, with a combination of the high photorefractivity and the role of SnO_2 as an efficient rare-earth luminescence sensitizer [1–3], SiO_2-SnO_2 glass-ceramics activated by rare-earth ions can be promising for constructing active optical integrated components, e.g. light sources and monolithic optical integrated circuits.

4. Conclusions

In this work, the high photorefractivity of SiO_2-SnO_2:Er^{3+} glass-ceramic planar waveguides was demonstrated. Under UV irradiation using a pulsed KrF excimer laser ($\lambda = 248$ nm), the SiO_2-SnO_2:Er^{3+} glass-ceramic planar waveguides showed a negative effective refractive index change. By increasing the SnO_2 content, a greater saturated effective refractive index change was obtained: $(2.6 \pm 0.2) \times 10^{-3}$ at 1550 nm on the TE_0 mode for 30 mol% SnO_2 planar waveguides and - $(2.0 \pm 0.2) \times 10^{-3}$ at 1550 nm on the 1550 nm TE_0 mode for the 20 mol% SnO_2 ones. In addition, the SiO_2-SnO_2:Er^{3+} glass-ceramic planar waveguides show a fast photorefractive response under UV irradiation. After a cumulative dose of only 0.3 kJ/cm^2, the 30 mol% SnO_2 planar waveguides reached their saturated effective refractive index change and the 20 mol% SnO_2 arrived at nearly 80% of their saturated value. The fluorescence background in the micro-Raman spectrum of the irradiated planar waveguides suggests that the network modification existing due to the presence of SnO_2 in SiO_2 matrix is involved in the photorefractive response of the material. Finally, the first result of a direct UV-written gratings fabrication using a CW frequency doubled argon laser ($\lambda = 244$ nm) on the highly photorefractive SiO_2-SnO_2:Er^{3+} planar waveguide was successfully demonstrated. Thanks to the fast photorefractive response of the SiO_2-SnO_2:Er^{3+} glass-ceramic planar waveguides, the energy density needed to obtain a refractive index change in the order of 10^{-3} was one order of magnitude less than the hydrogen loaded germanoborosilicate glasses. This suggests that, by exploiting the photorefractivity, the gratings fabrication on SiO_2-SnO_2:Er^{3+} glass-ceramic planar waveguides through the direct UV laser writing is less time-consuming. All the features reveal the outstanding photorefractive properties of SiO_2-SnO_2:Er^{3+} glass-ceramics, paving the way for an efficient top-down fabrication of optical devices (i.e.: channel waveguides and Bragg gratings) based on such binary systems for integrated optics.

Acknowledgements

The research activity is performed in the framework of the projects CNR-PAS “Flexible Photonics” (2020–2021), PRIN 2019 “NOMEN” (2020–2022).

Declaration of competing interest

The authors declare that they have no known competing financial interests or personal relationships that could have appeared to influence the work reported in this paper.

CRediT authorship contribution statement

Thi Ngoc Lam Tran: Investigation, Validation, Visualization, Writing - original draft. **Simone Berneschi:** Investigation, Validation. **Cosimo Trono:** Investigation, Validation. **Gualtiero Nunzi Conti:** Investigation, Validation. **Lidia Zur:** Investigation, Data curation, Writing - review & editing. **Cristina Armellini:** Resources. **Stefano Varas:** Resources. **Alessandro Carpentiero:** Resources. **Andrea Chiappini:** Investigation, Data curation, Writing - review & editing. **Alessandro Chiasera:** Investigation, Data curation, Writing - review & editing. **James Gates:** Investigation, Writing - review & editing. **Pier-John Sazio:** Investigation, Writing - review & editing. **Monica Bollani:** Funding acquisition, Project administration, Writing - review & editing. **Anna Lukowiak:** Supervision, Funding acquisition, Project administration, Writing - review & editing. **Giancarlo C. Righini:** Supervision, Funding acquisition, Project administration, Writing - review & editing. **Maurizio Ferrari:** Supervision, Funding acquisition, Project administration, Writing - review & editing.

References

[1] L. Zur, L.T.N. Tran, D. Massella, A. Vaccari, A. Chiappini, A. Chiasera, S. Varas, C. Armellini, A. Carpentiero, B. Boulard, D. Dorosz, S. Pelli, C. Trono, S. Berneschi, G.N. Conti, J. Gates, P.J. Sazio, B. Rossi, E. Iacob, V. Micheli, G. Speranza, G. Ischia, F. Prudenzano, A. Lukowiak, D. Zonta, R. Ramponi, G.C. Righini, M. Ferrari, SiO_2-SnO_2 transparent glass-ceramics activated by rare earth ions, Proc. SPIE Optical components and Materials XVI 10914 (2019), https://doi.org/10.1117/12.2507214, 10914–36.

[2] T.N.L. Tran, D. Massella, L. Zur, A. Chiasera, S. Varas, C. Armellini, C.G. Righini, A. Lukowiak, D. Zonta, M. Ferrari, SiO_2-SnO_2:Er^{3+} glass-ceramic monoliths, Appl. Sci. 8 (8) (2018) 1335, https://doi.org/10.3390/app8081335, 1-8.

[3] L. Zur, L.T.N. Tran, M. Meneghetti, V.T.T. Tran, A. Lukowiak, A. Chiasera, D. Zonta, M. Ferrari, G.C. Righini, Tin-dioxide nanocrystals as Er^{3+} luminescence sensitizers: formation of glass-ceramic thin films and their characterization, Opt. Mater. 63 (2017) 95–100, https://doi.org/10.1016/j.optmat.2016.08.041.

[4] A. Lukowiak, L. Zur, T.N.L. Tran, M. Meneghetti, S. Berneschi, G.N. Conti, S. Pelli, C. Trono, B.N.S. Bhaktha, D. Zonta, S. Taccheo, G.C. Righini, M. Ferrari, Sol–gel-derived glass-ceramic photorefractive films for photonic structures, Crystals 7 (61) (2017) 1–7, https://doi.org/10.3390/cryst7020061.

[5] S. Berneschi, B.N.S. Bhaktha, A. Chiappini, A. Chiasera, M. Ferrari, C. Kinowski, S. Turrell, C. Trono, M. Brenci, I. Cacciari, G.N. Conti, S. Pelli, G.C. Righini, Highly photorefractive Eu^{3+} activated sol-gel SiO_2-SnO_2 thin film waveguides, Proc. SPIE Integrated Optics: Devices, Materials, and Technologies XIV 7604 (2010) 76040Z, https://doi.org/10.1117/12.843210.

[6] C. Cascales, R. Balda, L. Lezama, J. Fernández, Site symmetry and host sensitization-dependence of Eu^{3+} real time luminescence in tin dioxide nanoparticles, Optic Express 26 (2018) 16155–16170, https://doi.org/10.1364/OE.26.016155.

[7] L. Zur, T.N.L. Tran, M. Meneghetti, M. Ferrari, Sol-gel derived SnO_2-based photonic systems, in: L. Klein, M. Aparicio, A. Jitianu (Eds.), Handbook of Sol-Gel Science and Technology, second ed., Springer International Publishing AG, Basel, Switzerland, 2017, pp. 1–19.

[8] L.T.N. Tran, D. Massella, R. Balda, S. Berneschi, W. Blanc, B. Boulard, A. Chiappini, A. Chiasera, P. Dentella, S. Eaton, J. Fernandez, M. Ferrari, J. Gates, P. Gluchowski, G. Ischia, A. Lukowiak, G.N. Conti, F. Prudenzano, B. Rossi, G.C. Righini, D. Zonta, L. Zur, SiO_2-SnO_2 photonic glass-ceramics, in: Proc. IEEE 21st International Conference on Transparent Optical Networks ICTON, 2019, https://doi.org/10.1109/ICTON.2019.8840012. We.C6.1.

[9] N. Chiodini, A. Paleari, G. Spinolo, P. Crespi, Photorefractivity in SiO_2:SnO_2 glass-ceramics by visible light, J. Non-Cryst. Solids 322 (1–3) (2003) 266–271, https://doi.org/10.1016/S0022-3093(03)00213-8.

[10] L. Dong, L. Reekie, M.G. Xu, D.N. Payne, J.L. Cruz, Enhanced photosensitivity in tin-codoped germanosilicate optical fibers, IEEE Photon. Technol. Lett. 7 (9) (1995) 1048–1050, https://doi.org/10.1364/OL.20.001982.

[11] L. Dong, J.L. Cruz, J.A. Tucknott, L. Reekie, D.N. Payne, Strong photosensitive gratings in tin-doped phosphosilicate optical fibers, Opt. Lett. 20 (19) (1995) 1982–1984, https://doi.org/10.1364/OL.20.001982.

[12] R. Laurence, D. Liang, Material considerations for Bragg fiber gratings, Proc. SPIE Photosensitive Optical Materials and Devices 2998 (1997) 2–10, https://doi.org/10.1117/12.264168.

[13] G. Brambilla, V. Pruneri, L. Reekie, Photorefractive index gratings in SnO_2:SiO_2 optical fibers, Appl. Phys. Lett. 76 (7) (2000) 807–809, https://doi.org/10.1063/1.125591.

[14] G. Brambilla, H. Rutt, Fiber Bragg gratings with enhanced thermal stability, Appl. Phys. Lett. 80 (18) (2002) 3259–3261, https://doi.org/10.1063/1.1475366.

[15] M. Majumder, T.K. Gangopadhyay, A.K. Chakraborty, K. Dasgupta, D. K. Bhattacharya, Fibre Bragg gratings in structural health monitoring-Present status and applications, Sens. Actuator A Phys. 147 (1) (2008) 150–164, https://doi.org/10.1016/j.sna.2008.04.008.

[16] Y. Yu, D. Chen, P. Huang, H. Lin, A. Yang, Y. Wang, Distribution-related luminescence of Eu^{3+} sensitized by SnO_2 nano-crystals embedding in oxide glassy matrix, J. Solid State Chem. 184 (2) (2011) 236–240, https://doi.org/10.1016/j.jssc.2010.11.021.

[17] A.F. Zatsepin, E.A. Buntov, V.S. Kortov, V.A. Pustovarov, H.J. Fitting, B. Schmidt, N.V. Gavrilov, Low-temperature photoluminescence of ion-implanted SiO_2:Sn^+ films and glasses, J. Surface Investigation. 6 (4) (2012) 668–672, https://doi.org/10.1134/S1027451012080198.

[18] T.T.T. Van, S. Turrell, M. Eddafi, B. Capoen, M. Bouazaoui, P. Roussel, S. Berneschi, G.C. Righini, M. Ferrari, S.N.B. Bhaktha, O. Cristini, C. Kinowski, Investigations of the effects of the growth of SnO_2 nanoparticles on the structural properties of glass-ceramic planar waveguides using Raman and FTIR spectroscopies, J. Mol. Struct. 976 (1–3) (2010) 314–319, https://doi.org/10.1016/j.molstruc.2010.04.010.

[19] B.N.S. Bhaktha, C. Kinowski, M. Bouazaoui, B. Capoen, O. Robbe-cristini, F. Beclin, P. Roussel, M. Ferrari, S. Turrell, Controlled growth of SnO_2 nanocrystals in Eu^{3+}-doped SiO_2 - SnO_2 planar waveguides: a spectroscopic investigation, J. Phys. Chem. C 113 (52) (2009) 21555–21559, https://doi.org/10.1021/jp907764p.

[20] A. Paleari, E. Franchina, N. Chiodini, A. Lauria, SnO_2 nanoparticles in silica: nanosized tools for femtosecond-laser machining of refractive index patterns, Appl. Phys. B Laser Optic. 88 (2006) 31912, https://doi.org/10.1063/1.2192579.

[21] A.C. Yanes, J. Méndez-Ramos, J. Del-Castillo, J.J. Velázquez, V.D. Rodríguez, Size-dependent luminescence of Sm^{3+} doped SnO_2 nano-particles dispersed in sol-gel silica glass, Appl. Phys. B Laser Optic. 101 (4) (2010) 849–854, https://doi.org/10.1007/s00340-010-4331-0.

[22] T.T.V. Tran, S. Turrell, B. Capoen, V.H. Le, M. Ferrari, R. Davor, L. Boussekey, C. Kinowski, Environment segregation of Er^{3+} emission in bulk sol-gel-derived SiO_2-SnO_2 glass ceramics, J. Mater. Sci. 49 (24) (2014) 8226–8233, https://doi.org/10.1007/s10853-014-8531-6.

[23] T.T.T. Van, S. Turrell, B. Capoen, L.Q. Vinh, O. Cristini-Robbe, M. Bouazaoui, F. D'Acapito, M. Ferrari, D. Ristic, A. Lukowiak, R. Almeida, L. Santos, C. Kinowski, Erbium-doped tin-silicate sol–gel-derived glass-ceramic thin films: effect of environment segregation on the Er^{3+} emission, Sci. Adv. Mater. 7 (2) (2015) 301–308, https://doi.org/10.1166/sam.2015.2022.

[24] B. Quang, N. Ngoc, T. Ngoc, N. Duc, Correlation between SnO_2 nanocrystals and optical properties of Eu^{3+} ions in SiO_2 matrix: relation of crystallinity, composition, and photoluminescence, J. Lumin. 163 (2015) 28–31, https://doi.org/10.1016/j.jlumin.2015.03.002.

[25] K. Gaff, A. Durandet, T. Weijers, J. Love, R. Boswell, Strong photosensitivity in tin-doped silica films, Electron. Lett. 36 (9) (2000) 842–843, https://doi.org/10.1049/el:20000574.

[26] N. Chiodini, A. Paleari, G. Brambilla, E.R. Taylor, Erbium doped nanostructured tin-silicate glass-ceramic composites, Appl. Phys. Lett. 80 (23) (2002) 4449–4451, https://doi.org/10.1063/1.1485105.

[27] N. Chiodini, A. Paleari, G. Spinolo, A. Chiasera, M. Ferrari, G. Brambilla, E. R. Taylor, Photosensitive erbium doped tin-silicate glass, J. Non-Cryst. Solids 311 (3) (2002) 217–222, https://doi.org/10.1016/S0022-3093(02)01419-9.

[28] N. Chiodini, S. Ghidini, A. Paleari, Mechanisms responsible for the ultraviolet photosensitivity of SnO_2-doped silica, Phys. Rev. B 64 (7) (2001), 073102, https://doi.org/10.1103/PhysRevB.64.073102.

[29] N. Chiodini, A. Paleari, G. Spinolo, Photorefractivity in nanostructured tin-silicate glass ceramics: a radiation-induced nanocluster size effect, Phys. Rev. Lett. 90 (5) (2003), 055507, https://doi.org/10.1103/PhysRevLett.90.055507.

[30] G.H. Chen, Y.G. Li, L.Y. Liu, Y.J. He, L. Xu, W.C. Wang, The photosensitivity and ultraviolet absorption change of Sn-doped silica film fabricated by modified chemical vapor deposition, J. Appl. Phys. 96 (11) (2004) 6153–6158, https://doi.org/10.1063/1.1809249.

[31] N. Chiodini, S. Ghidini, A. Paleari, G. Brambilla, V. Pruneri, Photoinduced processes in Sn-doped silica fiber preforms, Appl. Phys. Lett. 77 (23) (2000) 3701–3703, https://doi.org/10.1063/1.1330749.

[32] C. Sima, J.C. Gates, H.L. Rogers, P.L. Mennea, C. Holmes, M.N. Zervas, P.G. R. Smith, Ultra-wide detuning planar Bragg grating fabrication technique based on direct UV grating writing with electro-optic phase modulation, Optic Express 21 (13) (2013) 15747, https://doi.org/10.1364/OE.21.015747.